



HAL
open science

Al-Pd-Mn icosahedral quasicrystal: deformation mechanisms in the brittle domain.

Michael Texier, Anne Joulain, Joel Bonneville, Ludovic Thilly, Jacques Rabier

► To cite this version:

Michael Texier, Anne Joulain, Joel Bonneville, Ludovic Thilly, Jacques Rabier. Al-Pd-Mn icosahedral quasicrystal: deformation mechanisms in the brittle domain.. *Philosophical Magazine*, 2007, 87 (10), pp.1497-1511. 10.1080/14786430601047707. hal-00513797

HAL Id: hal-00513797

<https://hal.science/hal-00513797>

Submitted on 1 Sep 2010

HAL is a multi-disciplinary open access archive for the deposit and dissemination of scientific research documents, whether they are published or not. The documents may come from teaching and research institutions in France or abroad, or from public or private research centers.

L'archive ouverte pluridisciplinaire **HAL**, est destinée au dépôt et à la diffusion de documents scientifiques de niveau recherche, publiés ou non, émanant des établissements d'enseignement et de recherche français ou étrangers, des laboratoires publics ou privés.



Al-Pd-Mn icosahedral quasicrystal: deformation mechanisms in the brittle domain.

Journal:	<i>Philosophical Magazine & Philosophical Magazine Letters</i>
Manuscript ID:	TPHM-06-Aug-0318
Journal Selection:	Philosophical Magazine
Date Submitted by the Author:	28-Aug-2006
Complete List of Authors:	Texier, Michael; University Aix-Marseille III, Faculty of Sciences Joulain, Anne; Université de Poitiers, Laboratoire de Métallurgie Physique Bonneville, Joel; Université de Poitiers, Laboratoire de Métallurgie Physique Thilly, Ludovic; Université de Poitiers, Laboratoire de Métallurgie Physique Rabier, Jacques; Université de Poitiers, Laboratoire de Métallurgie Physique
Keywords:	quasicrystals, dislocations, plasticity
Keywords (user supplied):	core spreading, confining pressure



Al-Pd-Mn icosahedral quasicrystal: deformation mechanisms in the brittle domain.

MICHAEL TEXIER [†], ANNE JOULAIN [‡], JOEL BONNEVILLE ^{*‡}, LUDOVIC THILLY [‡],
JACQUES RABIER [‡]

[†] Université Aix-Marseille III, TECSEN, UMR-CNRS 6122, Case 262, Faculté des Sciences & Technologies de St Jérôme, 13397 Marseille Cedex 20, FRANCE.

[‡] Université de Poitiers, LMP, UMR-CNRS 6630, SP2MI, BP 30179, 86962 Chasseneuil Futuroscope Cedex, FRANCE.

The extreme brittleness of Al-Pd-Mn quasi-crystalline alloys over a wide range of temperatures drastically restricts the investigation of their plastic deformation mechanisms over a small high-temperature regime. Recently, plastic deformation of Al-Pd-Mn quasicrystal has been achieved in the brittle domain ($20^{\circ}\text{C} \leq T \leq 690^{\circ}\text{C}$) using specific deformation devices, which combined an uniaxial compression deformation or a shear deformation with an hydrostatic pressure confinement (0.35 GPa – 5 GPa). Results obtained with these experimental techniques, which provide various deformation conditions giving rise to a range of Al-Pd-Mn plastic features in the brittle domain, are discussed. On this basis, we propose that low and intermediate temperature plastic properties of Al-Pd-Mn are controlled by non-planar dislocation core extensions that are specific to the non-periodic structure.

Keywords: quasicrystal, dislocation, plasticity, core spreading, confining pressure.

* To whom correspondence should be addressed. E-mail: joel.bonneville@univ-poitiers.fr

§1.Introduction

The discovery of an ordered metallic phase with a non-periodic structure [1] induced a great interest in the scientific community. Quasiperiodic structures have been described using mathematical method [2,3] and appropriate indexation system has been built up for icosahedral quasicrystals [4]. Theoretical predictions of their structural defects and corresponding extinction conditions in transmission electron microscopy (TEM) were proposed [5] and verified by experimental observations [6].

The mechanical properties of quasicrystalline alloys are characterized by an extreme brittleness at low and intermediate temperatures, corresponding to a high brittle-to-ductile transition (BDT) temperature usually close to 70% of their melting temperature. This behaviour strongly suggests that diffusion plays an essential role in quasicrystal plasticity. Activation volumes, which were measured at high temperatures using different methods [7-11], have values too high to correspond to a deformation mechanism that would only imply diffusion. The stress-strain curves obtained at high temperatures for conventional deformation tests exhibit a yield point similar to the one observed in semi-conductors. For Si and Ge, the origin of the yield point has been ascribed to a lack of mobile dislocations [12], while for Al-Cu-Fe poly-quasicrystals it has been attributed to a lack of dislocation mobility [13]. Cottrell-Stokes type experiments [14] performed on Al-Cu-Fe [15] and Al-Pd-Mn [16,17] quasicrystals show that the flow stress is almost fully reversible with deformation temperatures, indicating that the variation of the applied stress with temperature essentially reflects the variation of the effective stress.

Dislocation activity has been observed in Al-Pd-Mn quasicrystalline thin foils deformed at high temperature during *in situ* TEM experiments [18], suggesting that plastic deformation may be ascribed to dislocation motion. However, the microscopic mechanism, by which dislocations move, has not been properly identified and the rate controlling mechanism is still a subject of debate. Previous observations of high-temperature deformed Al-Pd-Mn alloys concluded that dislocation motion essentially occurred by glide [19], whereas more recent studies of as-grown [20, 21] and deformed specimens [22] both give evidences of predominant climb processes.

These contradictory results deserve further study for identifying the microscopic deformation mechanism that controls quasicrystal plasticity. In particular, low

1
2
3 temperature deformation, *i.e.* when diffusion is unlikely to occur, may significantly
4 contribute to elucidate if pure dislocation glide can be initiated. Al-Pd-Mn specimens
5 were therefore deformed at low and intermediate temperatures, using experimental
6 techniques specifically designed for brittle materials, and the related microstructures
7 were examined by TEM. Special attention was paid to obtain from the *post mortem*
8 observations possible dislocation kinetics at the origin of the observed dislocation
9 configurations and to estimate the respective contribution of dislocation glide and
10 dislocation climb to plastic deformation. The peculiar plastic behaviour of Al-Pd-Mn is
11 explained and discussed in terms of a model based on non-planar core dislocation
12 configurations.

§.II. Experimental conditions

23
24
25
26
27
28 Poly-quasicrystals and mono-quasicrystals of nominal composition $\text{Al}_{66.3}\text{Pd}_{21.9}\text{Mn}_{11.8}$
29 and $\text{Al}_{70.5}\text{Pd}_{21.0}\text{Mn}_{8.5}$, respectively, were deformed under various deformation
30 conditions. Poly-quasicrystalline structure, which promotes homogeneous plastic
31 deformation for all deformation systems, was used in a first attempt to determine the
32 main characteristics of Al-Pd-Mn plasticity. The mono-quasicrystalline specimens, which
33 allow the initiation of plastic flow along particular directions and planes, were used to
34 verify special features suggested by the study of poly-quasicrystalline samples. For all
35 specimens, plastic deformation was applied via compression or shearing tests under
36 confining pressure produced either by a solid (multi-anvils, at 5 GPa) or gaseous
37 medium (Paterson press, at 300-400 MPa) to limit crack nucleation and propagation in
38 the brittle specimens. One must notice that stress-strain curves are only available for
39 the latter type of experiment. Performances and limitations of the various deformation
40 devices have been reported in detail in reference [23]. Compression and shearing tests
41 were performed at constant strain-rate, $\dot{\epsilon} = 1.5 \times 10^{-5} \text{ s}^{-1}$, over the temperature range
42 20 °C - 690 °C. Description of compression and shearing devices together with specimen
43 preparation and detailed deformation conditions can be found elsewhere [24, 25]; they
44 are summarised in table 1.

45
46
47
48
49
50
51
52
53
54
55
56
57
58
59
60
Thin foils for TEM were first cut from the deformed specimens using diamond
saw and subsequently thinned by ion milling at liquid nitrogen temperature. The

1
2
3 microstructures were observed in 'two-beam' conditions by TEM with a JEOL 200 CX
4 transmission electron microscope operating at 200 kV.
5
6
7

8 **§.III. Experimental results**

9 ***III.1. Macroscopic behaviour***

10
11
12
13
14
15
16 The stress-strain curves obtained from both the compression and the shearing tests
17 under gaseous confining pressure are similar to those obtained from conventional
18 deformation tests performed at high temperature and atmospheric pressure. After a few
19 percent of plastic strain, the applied stress reaches a maximum value, referred to as
20 σ_{UYS} , followed by a softening stage of continuous stress decrease. Examples of stress-
21 strain curves obtained for compression tests are presented in figure 1a, similar curves
22 for the shearing tests are available elsewhere [26].
23
24
25
26
27

28
29 The temperature dependence of σ_{UYS} is reported in figure 1b for the two types of
30 test, together with literature σ_{UYS} data obtained from conventional compression
31 experiments performed at high temperatures [27]. One can remark, except at 690 °C
32 where experimental difficulties were encountered (see figure 1a; the 690 °C
33 compression test was disturbed at 4% total strain by a temporary pressure leak leading
34 to an artefact in the load cell signal, as seen on the stress-strain curve), that the σ_{UYS} -T
35 dependence nicely follows a linear fit over a large temperature range, which for the
36 imposed strain-rate includes temperatures that belong to the brittle and ductile domains.
37 One should also note that a linear fit was also obtained only based on high temperature
38 results [28].
39
40
41
42
43
44
45
46
47

48 ***III.2. Microstructures***

49 ***III.2.1. Low temperature deformation ($T < 480$ °C)***

50
51
52
53
54
55 Detailed analyses of the low temperature deformation microstructures have already
56 been given elsewhere [24, 29, 30]. They can be summarized as follows.
57
58

59
60
61
62
63
64
65
66
67
68
69
70
71
72
73
74
75
76
77
78
79
80
81
82
83
84
85
86
87
88
89
90
91
92
93
94
95
96
97
98
99
100
101
102
103
104
105
106
107
108
109
110
111
112
113
114
115
116
117
118
119
120
121
122
123
124
125
126
127
128
129
130
131
132
133
134
135
136
137
138
139
140
141
142
143
144
145
146
147
148
149
150
151
152
153
154
155
156
157
158
159
160
161
162
163
164
165
166
167
168
169
170
171
172
173
174
175
176
177
178
179
180
181
182
183
184
185
186
187
188
189
190
191
192
193
194
195
196
197
198
199
200
201
202
203
204
205
206
207
208
209
210
211
212
213
214
215
216
217
218
219
220
221
222
223
224
225
226
227
228
229
230
231
232
233
234
235
236
237
238
239
240
241
242
243
244
245
246
247
248
249
250
251
252
253
254
255
256
257
258
259
260
261
262
263
264
265
266
267
268
269
270
271
272
273
274
275
276
277
278
279
280
281
282
283
284
285
286
287
288
289
290
291
292
293
294
295
296
297
298
299
300
301
302
303
304
305
306
307
308
309
310
311
312
313
314
315
316
317
318
319
320
321
322
323
324
325
326
327
328
329
330
331
332
333
334
335
336
337
338
339
340
341
342
343
344
345
346
347
348
349
350
351
352
353
354
355
356
357
358
359
360
361
362
363
364
365
366
367
368
369
370
371
372
373
374
375
376
377
378
379
380
381
382
383
384
385
386
387
388
389
390
391
392
393
394
395
396
397
398
399
400
401
402
403
404
405
406
407
408
409
410
411
412
413
414
415
416
417
418
419
420
421
422
423
424
425
426
427
428
429
430
431
432
433
434
435
436
437
438
439
440
441
442
443
444
445
446
447
448
449
450
451
452
453
454
455
456
457
458
459
460
461
462
463
464
465
466
467
468
469
470
471
472
473
474
475
476
477
478
479
480
481
482
483
484
485
486
487
488
489
490
491
492
493
494
495
496
497
498
499
500
501
502
503
504
505
506
507
508
509
510
511
512
513
514
515
516
517
518
519
520
521
522
523
524
525
526
527
528
529
530
531
532
533
534
535
536
537
538
539
540
541
542
543
544
545
546
547
548
549
550
551
552
553
554
555
556
557
558
559
560
561
562
563
564
565
566
567
568
569
570
571
572
573
574
575
576
577
578
579
580
581
582
583
584
585
586
587
588
589
590
591
592
593
594
595
596
597
598
599
600
601
602
603
604
605
606
607
608
609
610
611
612
613
614
615
616
617
618
619
620
621
622
623
624
625
626
627
628
629
630
631
632
633
634
635
636
637
638
639
640
641
642
643
644
645
646
647
648
649
650
651
652
653
654
655
656
657
658
659
660
661
662
663
664
665
666
667
668
669
670
671
672
673
674
675
676
677
678
679
680
681
682
683
684
685
686
687
688
689
690
691
692
693
694
695
696
697
698
699
700
701
702
703
704
705
706
707
708
709
710
711
712
713
714
715
716
717
718
719
720
721
722
723
724
725
726
727
728
729
730
731
732
733
734
735
736
737
738
739
740
741
742
743
744
745
746
747
748
749
750
751
752
753
754
755
756
757
758
759
760
761
762
763
764
765
766
767
768
769
770
771
772
773
774
775
776
777
778
779
780
781
782
783
784
785
786
787
788
789
790
791
792
793
794
795
796
797
798
799
800
801
802
803
804
805
806
807
808
809
810
811
812
813
814
815
816
817
818
819
820
821
822
823
824
825
826
827
828
829
830
831
832
833
834
835
836
837
838
839
840
841
842
843
844
845
846
847
848
849
850
851
852
853
854
855
856
857
858
859
860
861
862
863
864
865
866
867
868
869
870
871
872
873
874
875
876
877
878
879
880
881
882
883
884
885
886
887
888
889
890
891
892
893
894
895
896
897
898
899
900
901
902
903
904
905
906
907
908
909
910
911
912
913
914
915
916
917
918
919
920
921
922
923
924
925
926
927
928
929
930
931
932
933
934
935
936
937
938
939
940
941
942
943
944
945
946
947
948
949
950
951
952
953
954
955
956
957
958
959
960
961
962
963
964
965
966
967
968
969
970
971
972
973
974
975
976
977
978
979
980
981
982
983
984
985
986
987
988
989
990
991
992
993
994
995
996
997
998
999
1000

1
2
3 straight bands containing high dislocation densities characterize the microstructures.
4 Careful examination of the dislocations located at the tip of the bands indicates that they
5 predominantly have a screw character, their curvatures suggesting that they have
6 moved by glide in 5-fold planes. Planar defects bounded by partial dislocations are also
7 observed at all temperatures, with a density that clearly increases with increasing
8 temperature. Determination of fault habit planes together with related $b_{//}$ Burgers vector
9 directions indicates that these dislocations have moved either by climb or by a process
10 that involves a large climb component. In an attempt to check the stability of these
11 faults, *in situ* heating experiments of deformed specimens have been performed in
12 TEM. The planar faults were stable even after a heating of several tens of minutes at
13 700 °C.
14
15
16
17
18
19
20
21
22
23

24 III.2.2. Compression tests at intermediate temperatures ($480\text{ °C} \leq T \leq 690\text{ °C}$)

25
26
27

28 The dislocation microstructures of samples deformed at 480°C and 690°C exhibit some
29 common features, which are:

- 30 • dislocations are quite homogeneously distributed in the thin foils,
 - 31 • tri-dimensional networks of reacting dislocations are frequently observed,
 - 32 • dislocations are mainly located in 5-fold planes and show a segmented aspect, the
33 dislocation segments being preferentially oriented along two-fold directions,
 - 34 • dislocation dipoles are frequently observed. A complete description of such dislocation
35 dipoles has been given in [25].
 - 36 • isolated planar defects bounded by partials dislocations are still observed, but they are
37 quite rare and do not constitute anymore a dominant feature of the deformation
38 microstructures.
- 39
40
41
42
43
44
45
46
47

48 Figure 2a shows a typical example of segmented dislocations observed in
49 deformed specimens at 690°C. The dislocation density is rather low, suggesting that
50 their motion mainly results from the imposed stress and was not strongly influenced by
51 dislocation interactions. Different imaging conditions have been used for determining
52 their main characteristics. The rectilinear portions of each dislocation are aligned along
53 2-fold directions. The segment directions, labelled from 1 to 4 in figure 2a, lie in a
54 common five-fold plane, which is perpendicular to the compression axis. All dislocations
55 in figure 2a have the same extinction conditions. The physical component of their
56 Burgers vectors is found to be parallel to a 2-fold axis, inclined at 32° from the habit
57
58
59
60

1
2
3 plane normal. The dislocation segments have either a mixed character (segments 1 to
4 3) or a pure edge character (segment 4). It must be emphasised that, in contrast to low
5 deformation temperatures, no dislocation with a pure screw character has been
6 observed. Figure 2b is a schematic of one of the observed dislocation configurations in
7 figure 2a. The glide plane, defined by the line direction and the physical component $b_{//}$
8 of the Burgers vector, is shown for each segment. It can be seen that all segments,
9 which belong to the same five-fold plane, have different glide planes, forming a glide
10 cylinder. Note that this configuration leads to different Schmid factors for each
11 dislocation segments when glide is considered. Assuming that dislocation mobility for
12 glide is dependent on the plane of motion, this geometrical configuration strongly
13 suggests that the expansion of the dislocation loop occurred in the common five-fold
14 plane, which contains all the dislocation segments. Since $b_{//}$ makes an angle of 32° to
15 the normal of this plane, these dislocations have moved by a mechanism that includes a
16 large climb component.
17
18
19
20
21
22
23
24
25
26
27
28
29

30 *II.2.3. Shear experiments at intermediate temperatures ($480\text{ }^\circ\text{C} \leq T \leq 690\text{ }^\circ\text{C}$)*

31
32
33 The deformation microstructures of sheared mono-quasicrystalline specimens depend
34 strongly on the deformation temperature. The dislocation microstructure of specimens
35 sheared at $480\text{ }^\circ\text{C}$ is heterogeneously distributed within the thin foils, as confirmed by
36 the observation of specimen surfaces performed by scanning electron microscopy [26],
37 where some areas contain high densities of cracks. In these regions, no clear evidence
38 of dislocation activity is detected. Other zones, which certainly correspond to larger
39 shear amounts, are fragmented in numerous disoriented grains of few hundreds
40 nanometres in size (see Figure 3a). The corresponding selected area diffraction
41 patterns exhibit isolated spots distributed over discontinuous rings (see Figure 3b),
42 which confirm the small grain poly-quasicrystalline structure. It must be emphasized that
43 periodically aligned spots are observed (see for instance white arrows in figure 3b). This
44 bears witness to the presence of one or several grains with a crystalline structure. Since
45 the specimens were initially of highly perfect quasicrystalline phase [28], we conclude
46 that phase transformation has been induced by the deformation test. Pressure-induced
47 phase transformation has already been reported for bulk Al-Pd-Mn [31] and, more
48 recently, for nano-indented Al-Pd-Mn single quasicrystals [32].
49
50
51
52
53
54
55
56
57
58
59
60

1
2
3 The microstructure of specimen sheared at 690 °C presents similar
4 characteristics to the one obtained by compression at the same temperature. The
5 dislocation microstructure is homogeneously distributed in all the investigated thin foils.
6
7 Stereographic analyses indicate that the dislocations are contained in 5-fold planes, for
8 which the shear stress is maximum. Like for the dislocations observed in samples
9 deformed by compression test, a careful examination of the dislocation configurations
10 strongly suggest that their motion occurred by a climb process. Therefore, in spite of the
11 very favourable deformation conditions for promoting dislocation glide (shear plane
12 parallel to a 5-fold plane), no evidence of dislocation glide has been identified in the
13 specimens sheared at 480 °C and 690 °C.
14
15
16
17
18
19
20
21
22

23 §.IV. Discussion

24 25 26 *IV.1. Dislocation features*

27
28
29
30 With the exception of the specific case at room temperature, where screw dislocation
31 pile-ups are probably moving by glide, all other considered dislocation configurations
32 suggest that their formation results from dislocation movements that imply a
33 predominant climb component. In addition, experiments specifically designed for
34 promoting dislocation glide, *i.e.* shear experiment under high confining hydrostatic
35 pressure, failed to provide evidence of dislocation configurations that would result from
36 glide processes. Therefore, the present results confirm that dislocation glide is
37 extremely difficult to initiate in this quasicrystalline phase, at least for temperatures that
38 belong to the brittle domain. Nevertheless, on the basis of our observations only, we
39 cannot definitively conclude that dislocation glide does not take place in the icosahedral
40 phase, as was claimed for instance by others authors [33]. Dislocation motion may
41 strongly depend on the plane of motion, which would require a more extensive study
42 where not only 5-fold planes are preferentially favoured. In addition, the amount of
43 plastic strain may also have some importance, as explained below, and careful
44 investigations at various strain levels must be carried out.
45
46
47
48
49
50
51
52
53
54
55

56 The strong propensity of dislocations to move by non-conservative mechanisms
57 certainly constitutes the dominant characteristic of Al-Pd-Mn plasticity at low and
58 intermediate temperatures. In particular, diffusion processes are unexpected to occur at
59
60

1
2
3 such temperatures. Dislocation climb is usually expected to play an important role,
4 generally ascribed to dislocation microstructure recovery, when deformation
5 temperature reaches values higher than nearly one half of the melting temperature. In
6 the present case, dislocation climb does not contribute to dynamic recovery only but
7 also constitutes the main process by which plastic deformation is produced. This type of
8 climb-controlled plasticity is, in some aspects, similar to the one of the hexagonal
9 structure, such as Be and Mg, deformed under specific loading conditions [34].

10
11 The dislocation characteristics also exhibit some unexpected changes when the
12 deformation temperature is raised from low, *i.e.* typically room temperature, to
13 intermediate temperatures, *i.e.* essentially below the brittle-to-ductile transition
14 temperature. At low temperatures, some dislocations display characteristic typical fault
15 contrasts indicating that they participated to the plastic deformation. The fringe
16 contrasts associated with these planar defects do not vanish during *in situ* TEM heating
17 of deformed specimens, as observed for pure phasonic faults [35]. These planar defects
18 have a complex nature, which includes a topologic component in the quasiperiodic
19 stacking sequence together with a phasonic component. Consequently, these
20 dislocations are partial dislocations in the 6-dimensionnal (6D) space, *i.e.* their 6D
21 Burgers vectors are not translational vectors of the 6D periodic hyperlattice, E_{6D} . At
22 intermediate temperatures, dislocations bounding planar defects are very rare. As a
23 rule, the dislocations do not present fringe contrasts in their vicinity anymore, indicating
24 that they now have 6D Burgers vectors which are perfect translation vectors in E_{6D} . This
25 also indicates that the inherent phasonic faults dragged by moving dislocations have
26 been reordered during the deformation experiments, leading to the recovery of the
27 perfect icosahedral structure.

28
29 Another significant difference with increasing deformation temperature concerns
30 the shape of the dislocation lines, which evolves from curled aspects, with no
31 preferential orientation, at low temperatures to segmented configurations, with
32 dislocation segments aligned along particular quasi-crystallographic directions, at
33 intermediate temperatures. Three main hypotheses are usually proposed to explain the
34 latter dislocation shapes, which are:

- 35 • *elastic constant anisotropy* that leads to dislocation line alignments along energetically
36 favourable directions. However, the high isotropy of the icosahedral structure does not
37 support *a priori* such an assumption.
- 38
39
40
41
42
43
44
45
46
47
48
49
50
51
52
53
54
55
56
57
58
59
60

1
2
3 • *Peierls friction force*, the origin of which arises from the influence of the lattice
4 periodicity on a moving dislocation. In order to be efficient, this friction force
5 necessitates strong directional atomic bondings and leads to dislocation alignment
6 along specific directions that usually correspond to close-packed atomic directions. In
7 Al-Pd-Mn quasicrystals, such preferential directions are two-fold quasicrystallographic
8 axes. The segmented aspect is more and more pronounced with increasing
9 temperature and must be interpreted in connection with the viscous dislocation motion
10 observed during *in situ* TEM observations [18]. For a glide process, Peierls forces are
11 believed to be overcome by the thermally activated nucleation of kink pairs and the
12 subsequent sidewise motion of the kinks [36], akin to what has been proposed for
13 crystalline solids [37]. However in the present study, whatever the deformation
14 temperature is, dislocation motion always implies a climb component, ruling out this
15 classical description. The concept of Peierls forces [38] must be extended in the frame
16 of a non-conservative dislocation movement that replaces kink by jog, although the
17 concept of Peierls forces is not appropriate in the case of climb [P. Beauchamp,
18 private communication]. Since Al-Pd-Mn plasticity is climb controlled, dislocation
19 multiplication occurs through Bardeen-Herring type source, which precludes pre-
20 existing jogs and, therefore, requires jog pair nucleation. The similarity between kink
21 pair and jog pair nucleation and migration has been used to explain segmented
22 configuration [39]. In this description, a rectilinear dislocation aspect is obtained when
23 the time for jog pair nucleation is larger than the time for jog migration over distances
24 equal to the mean inter-jog spacing, whereas the reverse situation leads to curled
25 dislocations. The evolution of dislocation shapes from curled to segmented would
26 imply that jog-pair nucleation is, at low temperature, a process easier than jog
27 migration, with a reversal in the respective ease with which the two processes occur
28 with increasing temperatures. Based on the simple assumptions that both mechanisms
29 require diffusion and that only jog pair nucleation increases dislocation energy, one
30 should expect that, whatever the temperature is, jog pair nucleation is more difficult
31 than jog migration. In addition, dislocation cores can be seen as lines of easy diffusion,
32 similar to dislocation core in crystalline structure, and enhanced jog mobility. This
33 should be true particularly at low temperature, where bulk diffusion can be considered
34 as negligible. Consequently, while a competition between jog pair nucleation and jog
35 migration cannot be entirely refuted for explaining the dislocation shape and its
36 evolution with temperature, this interpretation appears rather unlikely.

1
2
3
4
5
6
7
8
9
10
11
12
13
14
15
16
17
18
19
20
21
22
23
24
25
26
27
28
29
30
31
32
33
34
35
36
37
38
39
40
41
42
43
44
45
46
47
48
49
50
51
52
53
54
55
56
57
58
59
60

- *dislocation core extensions* out of the plane of motion, in particular when dislocation core extends in more than one crystallographic plane. In this case, the dislocation tends to align along the common intersection line of the dissociation planes such as, for instance, screw dislocations in bcc crystals. Then, the segmented aspect results from energetically favourable dislocation configurations, which are similar, by some aspect, to Peierls valleys. However, dislocation dissociation in several planes yields sessile dislocation configurations, which are usually considered as impeding dislocation motion. In this description, we expect that an increase in core extension with increasing temperature would result in a decrease in dislocation mobility, which contrasts with the increasing dislocation activity observed when temperature is raised.

Nevertheless, as shown below, the temperature evolution of dislocation core gives a reasonable explanation for the evolution of dislocation shape with temperature.

IV.2. Interpretation of dislocation motion in icosahedral quasicrystals

IV.2.1. Displacement field associated with dislocations in quasicrystals

Dislocations can be introduced in quasicrystals by a generalization of the Volterra process in a 6-dimensional space, E_{6D} , where the full translational symmetry is obeyed. They can be described as singularities in the periodic hyperlattice, characterized by a 6D Burgers vector \vec{B} [5]. The 6D Burgers vector \vec{B} corresponds to the integration around the displacement field of the 6D hyperlattice, which can be separated into an elastic distortion ($b_{//}$) and a phason distortion (b_{\perp}). The complete displacement field of a dislocation may then be expressed as a function of $\vec{b}_{//}$ and \vec{b}_{\perp} , which describe the quasiperiodic lattice elastic distortion (phononic displacement field) and the rearrangement of quasiperiodic lattice nodes (phasonic displacement field), respectively. Since the quasicrystalline structure resulting from the 'cut and project' method does not depend on the choice of the origin in E_{\perp} , a shift of the projection space $E_{//}$ parallel to E_{\perp} has no effect on the overall quasicrystalline structure. However, a local displacement field in E_{\perp} leads to local tiling mismatch in $E_{//}$, that may have different nature (chemical, geometrical or both) depending on the position in $E_{//}$ where the displacement is applied. This displacement depends of the amplitude of \vec{b}_{\perp} with respect to the atomic surface extension in E_{\perp} , which varies according to its position in $E_{//}$.

1
2
3 Therefore, the total displacement field in $E_{//}$ due to a dislocation line can be written as
4 the sum of a constant component $\vec{u}_{//, \vec{b}_{//}}$, which is proportional to $\vec{b}_{//}$ and a component
5 $\vec{u}_{//, \vec{b}_{\perp}}$, which varies in direction and amplitude along the dislocation line in $E_{//}$.
6
7

8
9 An analogy of dislocation displacement field in quasicrystals can be made with the
10 scheme of topological linear defect in solids proposed by Somigliana [40, 41]. In this
11 treatment, linear defects are produced by joining the two surfaces of a cut cylinder,
12 where the two surfaces have been independently deformed prior to the translation along
13 the cut surface. The resulting defects are not characterized by a constant displacement
14 vector as in the case of a Volterra's dislocations: the magnitude and direction of the
15 Burgers vector of these dislocations both fluctuate about an average value $\langle \vec{b} \rangle$, which
16 depends on the local surrounding material structure. The displacement field is then
17 described by the sum of a constant Burgers vector component, $\langle \vec{b} \rangle$, and a variable
18 component, arising from localised dislocation loops, which accounts for local
19 fluctuations of the total Burgers vector. In the quasicrystalline structure, the local
20 Burgers vector corresponds to the sum of the $\vec{b}_{//}$ component and a variable component,
21 which represents, in the physical space, the phasonic displacements due to the \vec{b}_{\perp}
22 component. Since the atomic displacements due to this variable component have an
23 equal probability to occur in all directions, the comparison of both dislocation
24 descriptions leads to assimilate $\langle \vec{b} \rangle$ in amorphous solids to the $\vec{b}_{//}$ component in
25 quasicrystalline structures. In amorphous solids, the motion of dislocations with non-
26 constant Burgers vectors implies the nucleation of small prismatic dislocation loops in
27 front and/or in the wake of the moving dislocation [42], in a similar way as phasons are
28 created in quasicrystals. Like phasons in the case of quasicrystals, the dislocation loops
29 do not directly participate to plastic deformation, but allow accomodating the geometric
30 mismatch between the two interfaces in translation. As a consequence, the deformation
31 is confined to narrow deformation bands, which contain the loops, phasons here,
32 produced by the first moving dislocation. This collective dislocation behaviour is usually
33 associated with a yield point on the σ - ε curves obtained for compression tests
34 performed at constant strain-rate. It also leads to very localised plastic deformation
35 events corresponding to small activation volumes and, in a correlative manner, to a high
36 temperature sensitivity of the yield stress. Amorphous and quasicrystalline materials
37 share all these characteristics.
38
39
40
41
42
43
44
45
46
47
48
49
50
51
52
53
54
55
56
57
58
59
60

IV.2.2. Dislocation behaviour

The variable component of the displacement field can produce a variety of atomic displacements along the dislocation line, which for energetic reasons may lead to a spreading of the dislocation core. In Al-Pd-Mn, TEM observations suggest that dislocations have non-planar cores that belong to the “climb” class, as classified in [43]. In this case, the dislocation core spreads into several planes, which belong to the zone of the vector parallel to the dislocation line. The Burgers vectors of the fractional dislocations involved in the core spreading possess components that are perpendicular to spreading planes. The existence of climb cores has been reported in several materials [44-49]. Such dissociations usually imply severe restrictions to dislocation movement, in particular when the temperature is decreased to the level at which dislocation climb is inhibited.

Climb core extension is supposed to influence only edge and mixed dislocation motions and cannot be applied to screw dislocation, for which motion occurs by glide only. It must be noticed that the mobility of screw dislocations can be strongly limited by sessile core extensions. For given projection conditions, the volume extensions of dislocation core are function of the dislocation position in E_{6D} and of the Burgers vector ratio ξ , where $\xi = |b_{\perp}|/|b_{\parallel}|$. This implies that the motion and the mobility of dislocations are both dependent on their ξ values. As a consequence, the densities of dislocations characterized by different ξ parameters should evolve during plastic deformation, leading to an increase in the density of dislocations with the most energetically favourable ξ ratio. For ξ ratio lower than a critical value ξ_c , dislocation movements are controlled by core extensions that do not favour either climb or glide mechanisms, whereas for higher ξ values dislocation climb is strongly enhanced, due to high anisotropic core extensions outside the glide plane as depicted in figure 4. This interpretation is in agreement with the observed evolution in dislocation densities with plastic strain characterized by different ξ values [27, 49].

From TEM observations of dislocation microstructures performed on specimens deformed at high temperatures [27, 49], it appears reasonable to assume that $\xi_c = \tau^5$ corresponds to the critical value above which dislocation motion is restricted to climb. At all temperatures, dislocation core extensions outside the glide plane confine dislocation

1
2
3 motion in or near the climb plane, in agreement with the observed dislocation
4 configurations [25, 29, 33].

5
6 Dislocation core extensions, which are assumed to result from geometrically necessary
7 atomic displacements along the dislocation line, are dependent on the geometrical
8 disorder of the quasicrystalline structure. The existence of a displacement field
9 component $\vec{u}_{//}, \vec{b}_{\perp}$ corresponds to a decrease in the dislocation misfit energy by partial
10 relaxation the local mismatch produced by the constant $\vec{u}_{//}, \vec{b}_{//}$ component of the perfect
11 quasicrystalline structure. Thus, the contribution of $\vec{u}_{//}, \vec{b}_{\perp}$ with temperature may be
12 significantly reduced by the presence of a higher phasonic defect density. In that case,
13 the amplitude of the core extensions out of the glide plane is reduced. Assuming that
14 the variations in elastic and misfit energies of dislocations in quasicrystals are similar to
15 the ones in crystalline structures [38, 50], the decrease of the core extension in the
16 climb plane yields an increase of the total dislocation energy. This results in a small
17 core spreading in the glide plane, leading to some kind of Peierls forces acting on the
18 dislocation line in the climb plane, which are believed to be at the origin of the observed
19 segmented dislocation configurations.

20
21 Since vacancy diffusion, which increases exponentially with temperature,
22 contributes to phasonic defect nucleation and propagation (as schematised in figure 5);
23 an increasing disorder is therefore expected at high temperature, leading to higher
24 dislocation segmentation when temperature is raised.

25 26 27 28 29 30 31 32 33 34 35 36 37 38 39 40 41 **§ V. Conclusion**

42
43
44 In this study, experimental techniques using confining pressure were used to
45 characterise the plastic behaviour of Al-Pd-Mn icosahedral quasicrystals in the brittle
46 domain. At room temperature, dislocation glide is evidenced, but for all deformation
47 temperatures below the BTD temperature, dislocation climb is identified. Above room
48 temperature, this mechanism becomes rapidly predominant with increasing
49 temperatures. At temperatures close to the BTD temperature, dislocations exhibit
50 segmented aspects. This feature is also observed for higher deformation temperatures.
51 We propose that low and intermediate temperature dislocation climb and segmented
52 dislocations have a common origin: a non-planar dislocation core extension, which
53 inhibits dislocation glide and, to a lesser degree, dislocation climb. This non-planar core
54
55
56
57
58
59
60

1
2
3 extension, specific to the non-periodic structure, is assumed to evolve with strain and
4 temperature concomitantly with phasonic defect concentration.
5
6
7
8
9

10 Acknowledgments

11
12
13 The authors are indebted to Dr. M. Feuerbacher for providing Al-Pd-Mn single
14 quasicrystals. Pr P. Guyot is gratefully acknowledged for helpful discussions. 'Région
15 Poitou-Charentes' is also acknowledged for financial support.
16
17
18
19
20
21
22

23 References

- 24
25
26 [1] Shechtman, D., Blech, I., Gratias, D., Cahn, J.W., *Phys. Rev. Lett.*, **53**, 1951
27 (1984).
28
29 [2] Levine, D., Steinhardt, P.J., *Phys. Rev. Lett.*, **53**, 2477 (1984).
30
31 [3] Levine, D., Steinhardt, P.J., *Phys. Rev. B.*, **34**, 596 (1986).
32
33 [4] Cahn, J.W., Shechtman, D., Gratias, D., *J. Mater. Res.*, **1**, 13 (1986).
34
35 [5] Wollgarten, M., Gratias, D., Zhang, Z., Urban, K., *Phil. Mag. A*, **64**, 819 (1991).
36
37 [6] Wollgarten, M., Zhang, Z., Urban, K., *Phil. Mag. Lett.*, **65**, 1 (1992).
38
39 [7] Takeuchi, S., Hashimoto, T., *Jpn. J. Appl. Phys.*, **32**, 2063 (1993).
40
41 [8] Bresson, L., Gratias, D., *J. Non-Cryst. Sol.*, **153-154**, 478 (1993).
42
43 [9] Brunner, D., Plachke, D., Carstnjen, H.D., *Mat. Sci. & Eng. A*, **234-236**, 310
44 (1997).
45
46 [10] Giacometti, E., Baluc, N., Bonneville, J., *Phil. Mag. Lett.*, **79**, 1 (1999).
47
48 [11] Texier, M., Prout, A., Bonneville, J., *Mat. Sci. & Eng. A*, **400-401**, 315 (2005).
49
50 [12] Omri, M., Tete, C., Michel J. P., George, A., *Phil. Mag. A* **55**, 5 (1987).
51
52 [13] Texier, M., Bonneville, J., Prout, A., Rabier, J., Baluc, N., Guyot, P., *Scripta*
53 *Materialia*, **49**, 41 (2003).
54
55 [14] Cottrell, A. H., Stockes, R.J., *Proc. Roy. Soc. A*, **233**, 17 (1955).
56
57 [15] Giacometti, E., Baluc, N., Bonneville, J., *proc. MRS Winter meeting 1998*,
58 Boston, Massachusetts, ed. Dubois, J.-M, Thiel, P.A., Tsai, A.-P., Urban, K.,
59 Materials Research Society, Boston, **553**, p295 (1999).
60

- 1
2
3 [16] Feuerbacher, M., Baufeld, B., Rosenfeld, R., Bartsch, M., Hanke, G., Beyss, M.,
4 Wollgarten, M., Messerschmidt, U., Urban, K., *Phil. Mag. Lett.*, **71**, 91 (1995).
5
6 [17] Brunner, D., Plachke, D., Carstnjen, H.D., *Mat. Sci. & Eng. A*, **234-236**, 310
7 (1997).
8
9 [18] Wollgarten, M., Beyss, M., Urban, K., Liebertz, H., Köster, U., *Phys. Rev. Lett.*,
10 **71**, 549 (1993).
11
12 [19] Wollgarten, M., Bartsch, M., Messerschmidt, U., Feuerbacher, M., Rosenfeld, R.,
13 Beyss, M., Urban, K., *Phil. Mag. Lett.*, **71**, 99 (1995).
14
15 [20] Shield, J.E., Kramer, M.J., McCallum, R.W., *J. Mater. Res.* **9**, 343 (1994).
16
17 [21] Caillard, D., Vanderschaeve, G., Bresson, L., Gratias, D., *Phil. Mag. A.*, **80**, 1,
18 237 (2000).
19
20 [22] Caillard, D., Roucau, C., Bresson, L., Gratias, D., *Acta Mat.*, 50, 4499 (2002).
21
22 [23] Fikar, J., Bonneville, J., Rabier, J., Baluc, N., Prout, A., Cordier, P., Stretton, I. in
23 *symposium Quasicrystals*, Proc. Materials Research Society Symposium, **643**,
24 K.7.4.1 (2001).
25
26 [24] Texier, M., Prout, A., Bonneville, J., Rabier, J., Baluc, N., Cordier, P., *Phil. Mag.*
27 *Lett.*, **82**, 659 (2002).
28
29 [25] Texier, M., Bonneville, J., Prout, A., Rabier, J., Thilly, L., *Materials Research*
30 *Society Symposium Proceedings*, **805**, LL.5.3.1 (2004).
31
32 [26] Texier, M., Thilly, L., Bonneville, J., Prout, A., Rabier, J., *Mat. Sci. & Eng. A*, **400-**
33 **401**, 311 (2005).
34
35 [27] Feuerbacher, M., Metzmacher, C., Wollgarten, M., Urban, K., Baufeld, B.,
36 Bartsch, M., Messerschmidt, U., *Mat. Sci. & Eng. A*, **233**, 103 (1997).
37
38 [28] Feuerbacher, M., Klein, H., Bartsch, M., Messerschmidt, U., Urban, K., *Mat. Sci.*
39 *& Eng. A.*, **294-296**, 736 (2000).
40
41 [29] Texier, M., Prout, A., Bonneville, J., Rabier, J., Baluc, N., Cordier P., *Scripta*
42 *Materialia*, **49**, 47 (2003).
43
44 [30] Texier, M., Prout, A., Bonneville, J., Rabier, J., *Mat. Sci. & Eng. A*, **387-389**,
45 1023 (2004).
46
47 [31] Baluc, N., Peyronneau, J., Kléman, M., *Proc. ICEM 13 Paris*, 491 (1994).
48
49 [32] Coupeau, C., Texier, M., Joulain, A., Bonneville, J., *Appl. Phys. Let.* **88** 073103
50 (2006).
51
52 [33] Mompou, F., Caillard, D., *Materials Research Society Symposium Proceedings*,
53 **805**, LL.5.4.1 (2004).
54
55
56
57
58
59
60

- 1
2
3 [34] Edelin, G., Poirier, J.P., *Phil. Mag.* **28**, 1203&1211 (1973).
4
5 [35] Takeuchi, S., Hashimoto, T., *Jpn. J. Appl. Phys.*, **32**, 2063 (1993).
6
7 [36] Takeuchi, S., Tamura, R., Kabutoya, E., Edagawa, K., *Phil. Mag. A*, **82**, 379
8 (2002).
9
10 [37] Seeger, A., Schiller, P., *Physical Acoustics, Principles and methods*, vol III, part
11 A, ed. Mason W.P., Academic press, New York, p448 (1966).
12
13 [38] Hirth, J.P., Lothe, J., *Theory of dislocations*, ed. Bever M.B., Shank M.E., Wert C.
14 A., Mehl R.F., McGraw-Hill Series (1982).
15
16 [39] Momprou, F., Caillard. D., Feuerbacher, M., *Phil. Mag.*, **84**, 25-26, 2777 (2004).
17
18 [40] Somigliana, C., *Atti Accad. Naz. Lincei Rc.*, **23**, 463 (1912).
19
20 [41] Somigliana, C., *Atti Accad. Naz. Lincei Rc.*, **24**, 655 (1915).
21
22 [42] Escaig, B., *Dislocations et déformation plastique*, ed. Groh P., Kubin L.P., Martin
23 J.-L., EDP, Yrivals, p. 261 (1979).
24
25 [43] Vitek, V., *Dislocations and Properties of Real Materials*, the Inst. of Met., London,
26 p. 30 (1985).
27
28 [44] Stohr, J.F., Poirier, J.P., *Phil. Mag.* **25**, 1313 (1972).
29
30 [45] Veysière, P., *Phil. Mag. A* **50**, 189 (1984).
31
32 [46] Douin, J., Beauchamp, P., Veysière, P., *Phil. Mag. A* **58**, 923 (1988).
33
34 [47] Duclos, R., Doukhan, N., Escaig, B., *J. Mat. Sci.* **13**, 1740 (1978).
35
36 [48] Lagerlof, K.D.P., Mitchell, T.E., Heur, A.H., Rivière, Cadoz, J., Castaing, J.,
37 Philips D.J., *Acta Metall.* **32**, 97 (1984).
38
39 [49] Schall, P., Feuerbacher, M., Bartsch, M., Messerschmidt, U., Urban, K., *Mat. Sci.*
40 *& Eng. A* **294-296**, 765 (2000).
41
42 [50] Philibert, J., *Dislocations et déformation plastique*, ed. Groh P., Kubin L.P.,
43 Martin J.-L., EDP, Yrivals, p101 (1979).
44
45
46
47
48
49
50
51
52
53
54
55
56
57
58
59
60

Table caption

Table 1 : Deformation parameters of the various deformation tests (*C*: composition in at. %, *D. T.* : deformation type, *T*: temperature in °C, *C. M.*: confining medium, *p*: hydrostatic confining pressure in GPa, *ε* : permanent strain after testing in %).

<i>Samples</i>	<i>C (in at. %)</i>	<i>D.T.</i>	<i>T (°C)</i>	<i>C. M.</i>	<i>p (GPa)</i>	<i>ε (%)</i>
Poly-grained	Al _{66.3} Pd _{21.9} Mn _{11.8}	compression	20	Solid	5	~ 6
Poly-grained	Al _{66.3} Pd _{21.9} Mn _{11.8}	compression	150	solid	5	~ 6
Poly-grained	Al _{66.3} Pd _{21.9} Mn _{11.8}	compression	300	solid	5	~ 6
Single-grained	Al _{70.5} Pd _{21.0} Mn _{8.5}	compression	480	gaseous	0.36	~ 5
Poly-grained	Al _{66.3} Pd _{21.9} Mn _{11.8}	compression	580	gaseous	0.35	~ 6.5
Poly-grained	Al _{66.3} Pd _{21.9} Mn _{11.8}	compression	610	gaseous	0.35	~ 6
Single-grained	Al _{70.5} Pd _{21.0} Mn _{8.5}	compression	690	gaseous	0.35	~ 6.5
Single-grained	Al _{70.5} Pd _{21.0} Mn _{8.5}	shear	480	gaseous	0.36	>20
Single-grained	Al _{70.5} Pd _{21.0} Mn _{8.5}	shear	690	gaseous	0.3	>20

TABLE 1

Figure captions

Figure 1. a) Stress-strain curves obtained during compression tests under a gaseous confining pressure of 0.35 GPa. b) Upper yield stress, σ_{UYS} , as a function of temperature: (o) uniaxial compression tests and (x) shear tests obtained under confining pressure, (■) conventional compression tests at atmospheric pressure (from [27]).

Figure 2. a) Example of dislocations observed in a specimen deformed at 690 °C. All dislocation segments are aligned along 2-fold directions. b) Schematic of the corresponding dislocation configuration. Dislocation segments are lying in a common 5-fold plane, but belong to different glide planes: dislocation segments (1) and (2) have two distinct 3-fold glide planes, segment (3) has a 5-fold glide plane.

Figure 3. a) Microstructure of a specimen sheared at 480 °C. A microstructure with small disoriented grains is observed. b) Related selected area electron diffraction pattern. The arrows indicate periodically aligned spots.

Figure 4. Schematic of expected ξ dependences of dislocation core extensions:

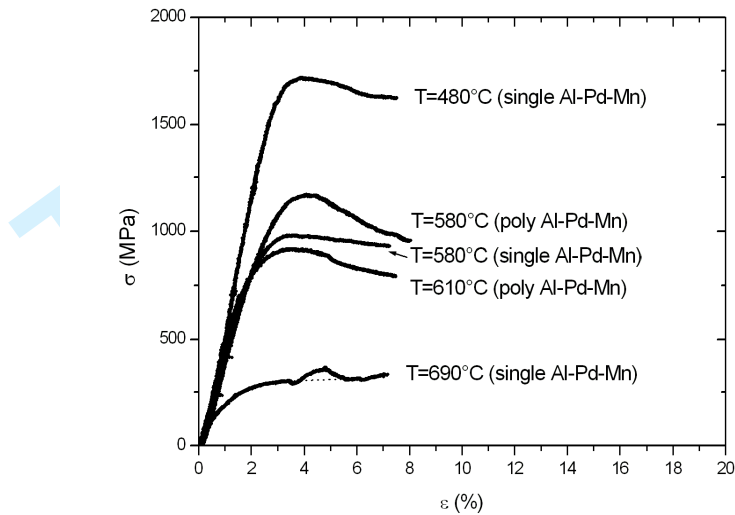
a) Low temperatures.

- for low ξ values, $\vec{u}_{//, b_{//}}$ and $\vec{u}_{//, b_{\perp}}$ displacement fields are similar, leading to almost equivalent core extensions in the glide and climb planes.
- for high ξ values, extensions out of the glide plane are predominant, promoting dislocation climb.

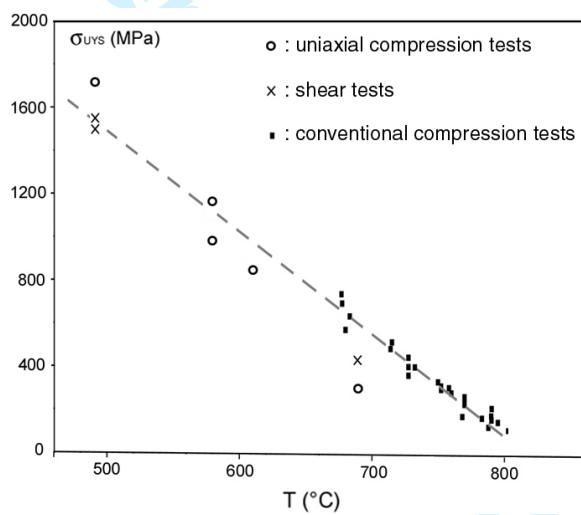
1
2
3 b) High temperatures. With increasing temperatures, due to the phasonic displacement
4 field, the geometrically necessary atomic displacements are reduced, leading to a
5
6 decreasing core extension in the climb plane.
7
8
9

10
11
12 **Figure 5.** Diffusion of a vacancy in a 2D-quasiperiodic structure: (a) the vacancy (open
13 square) occupies a node site of the quasiperiodic lattice. (b) The vacancy and one atom
14 exchange their sites. (c) The vacancy moves away to another position of the quasi-
15 lattice, but the atom sits at an intermediate position (open circle). This site does not
16 correspond to an actual node position of the perfect quasiperiodic lattice and represents
17 a so-called phasonic defect, referred to as 'basculon'. In that case, vacancy diffusion
18 enhances phasonic defect nucleation, allowing a reduction in the atomic flux associated
19 with vacancy migration.
20
21
22
23
24
25
26
27
28
29
30
31
32
33
34
35
36
37
38
39
40
41
42
43
44
45
46
47
48
49
50
51
52
53
54
55
56
57
58
59
60

1
2
3
4
5
6
7
8
9
10
11
12
13
14
15
16
17
18
19
20
21
22
23
24
25
26
27
28
29
30
31
32
33
34
35
36
37
38
39
40
41
42
43
44
45
46
47
48
49
50
51
52
53
54
55
56
57
58
59
60



a)



b)

FIGURE 1

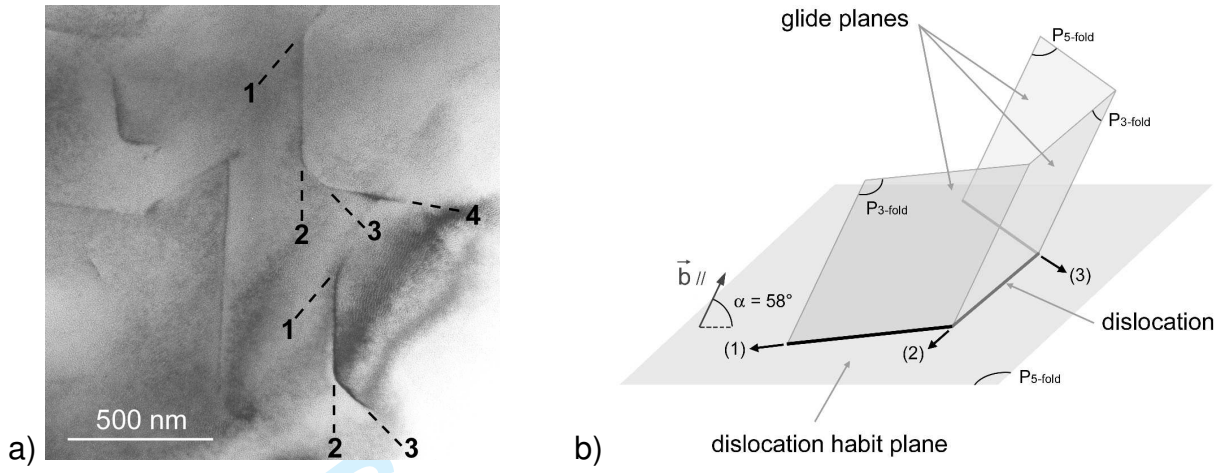


FIGURE 2

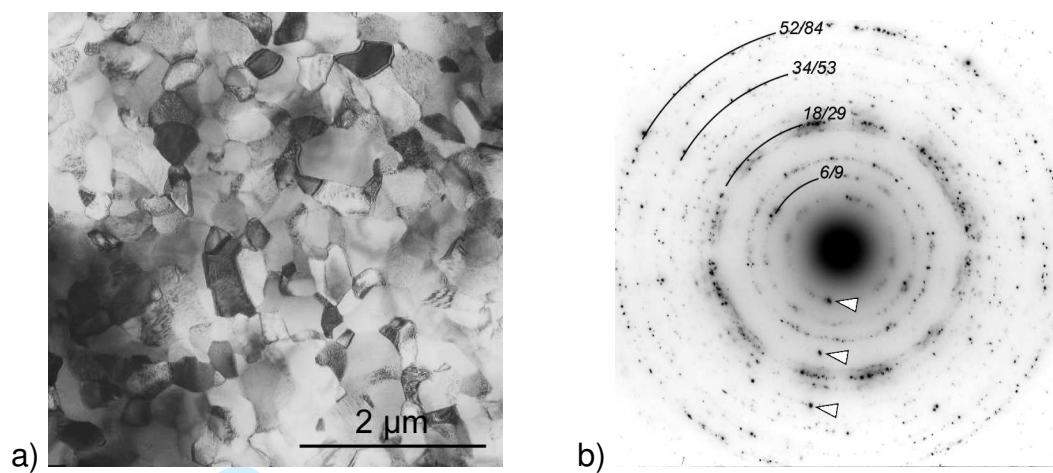


FIGURE 3

1
2
3
4
5
6
7
8
9
10
11
12
13
14
15
16
17
18
19
20
21
22
23
24
25
26
27
28
29
30
31
32
33
34
35
36
37
38
39
40
41
42
43
44
45
46
47
48
49
50
51
52
53
54
55
56
57
58
59
60

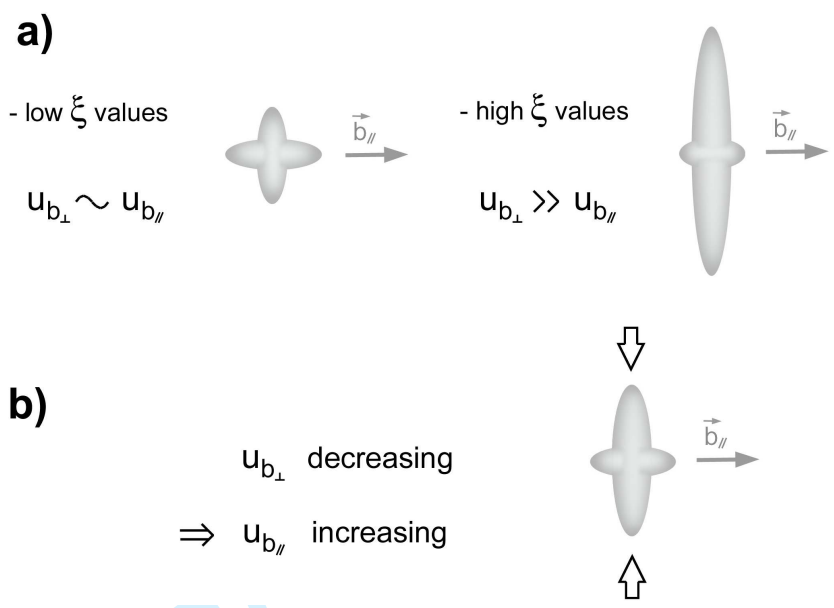


FIGURE 4

Peer Review Only

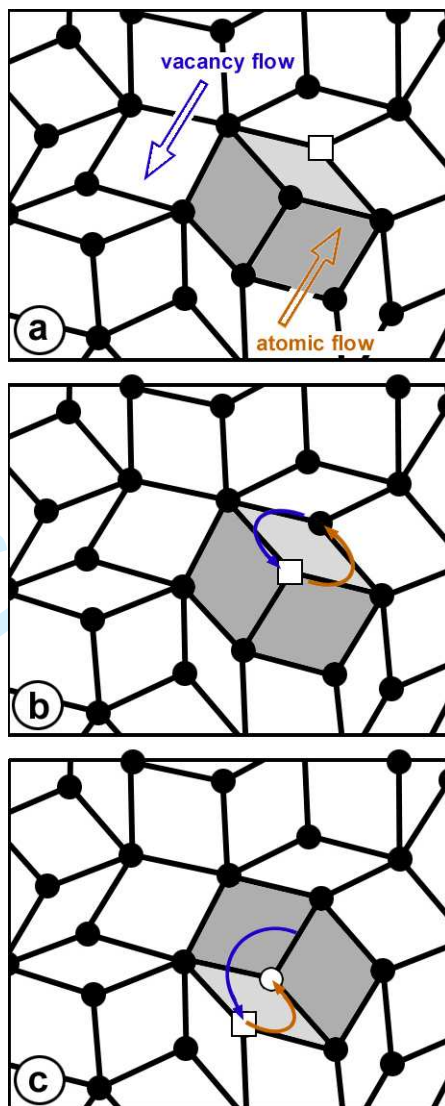
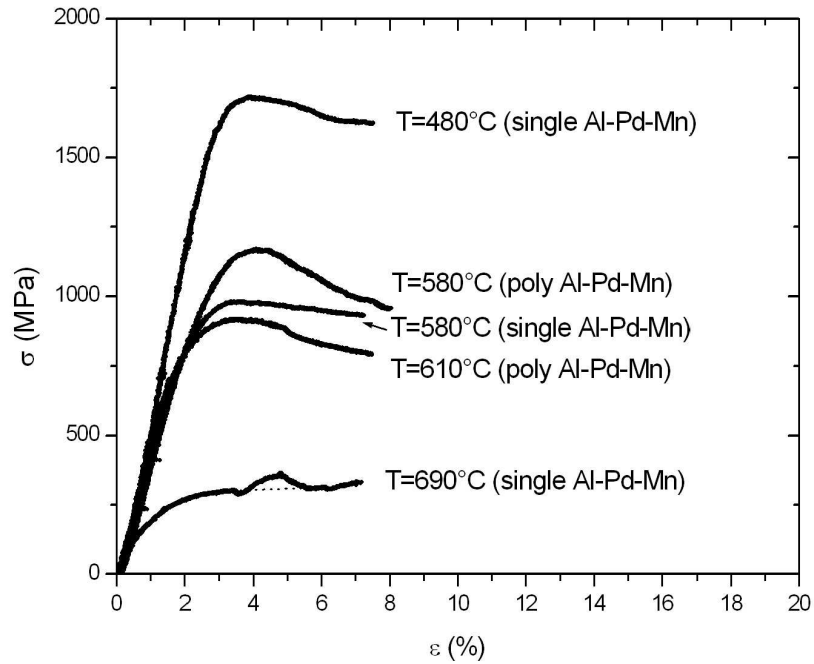
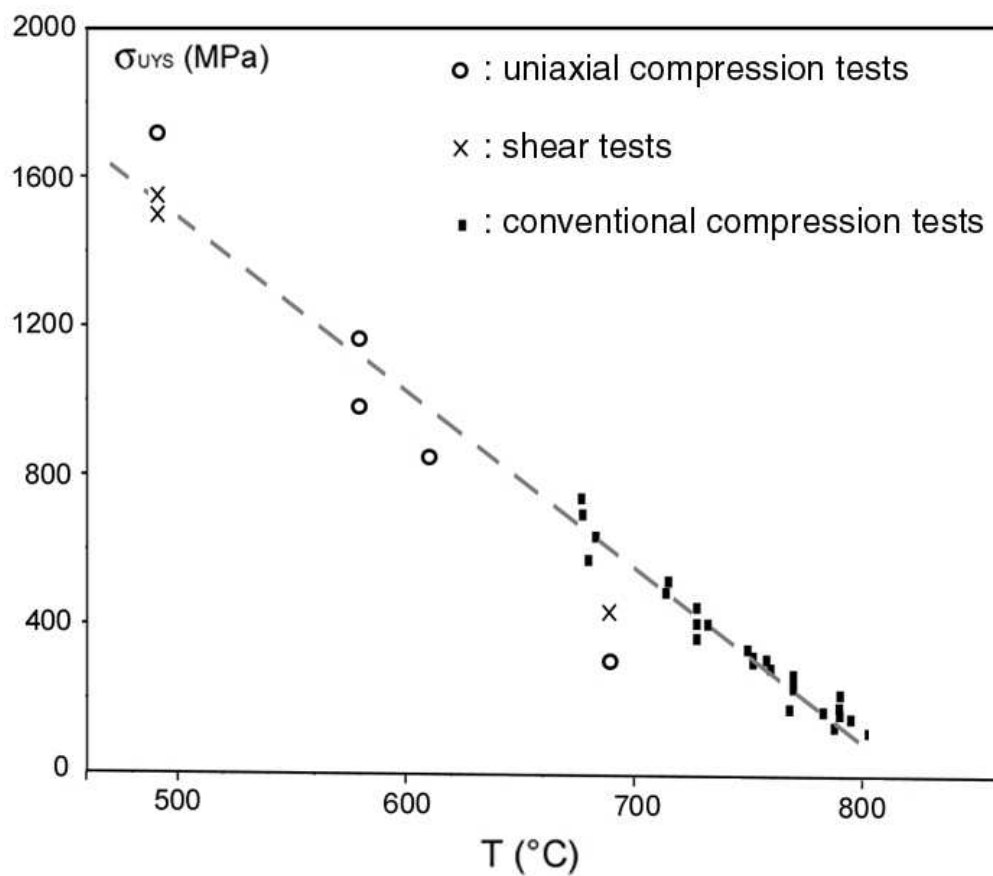


FIGURE 5



Stress-strain curves obtained during compression tests under a gaseous confining pressure of 0.35 GPa.

279x215mm (150 x 150 DPI)

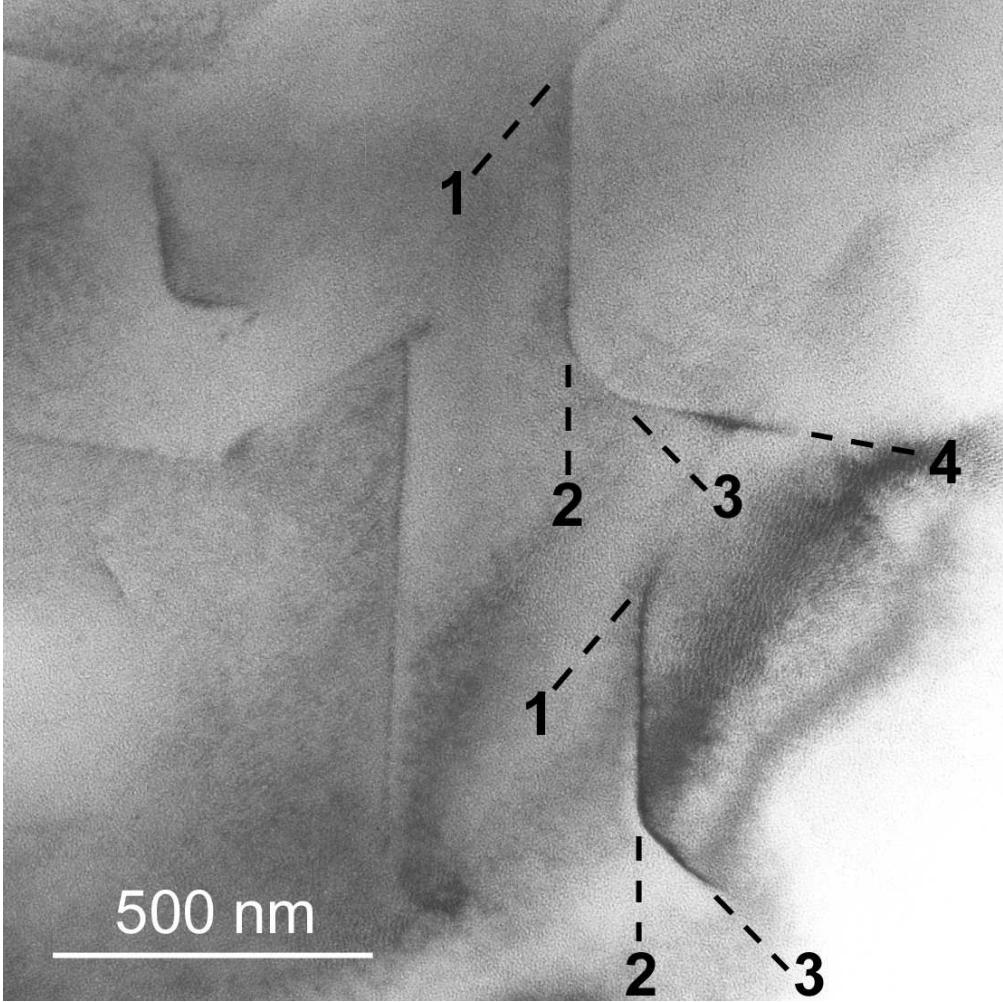


Upper yield stress, σ_{UYS} , as a function of temperature: (○) uniaxial compression tests and (×) shear tests obtained under confining pressure, (■) conventional compression tests at atmospheric pressure (from [27]).

114x99mm (154 x 154 DPI)

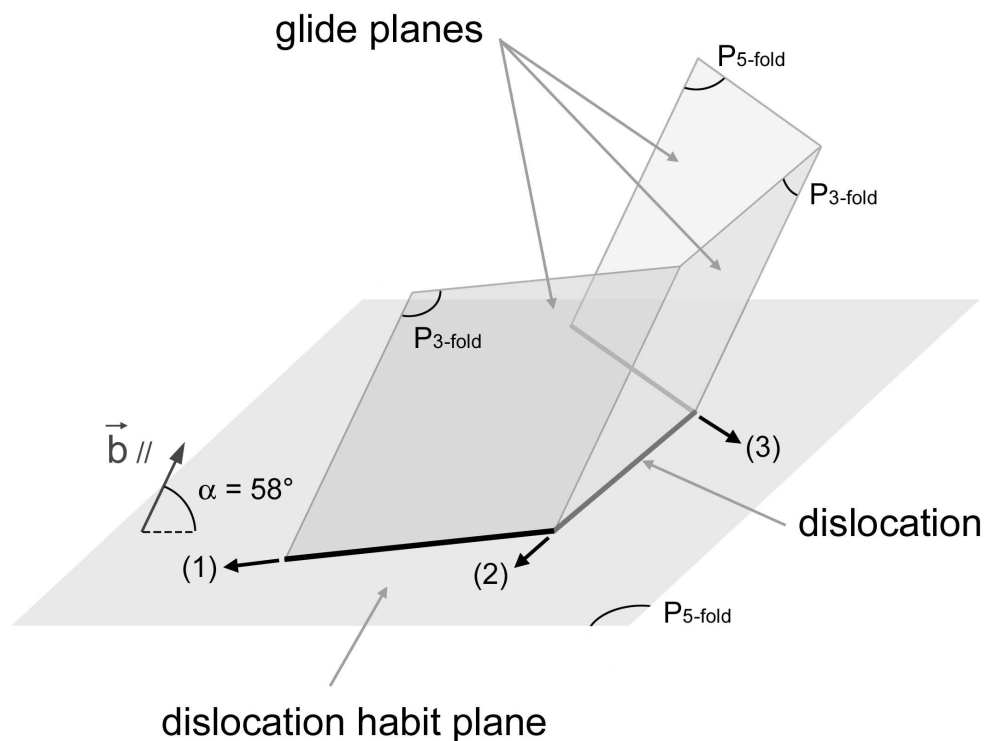
Only

1
2
3
4
5
6
7
8
9
10
11
12
13
14
15
16
17
18
19
20
21
22
23
24
25
26
27
28
29
30
31
32
33
34
35
36
37
38
39
40
41
42
43
44
45
46
47
48
49
50
51
52
53
54
55
56
57
58
59
60



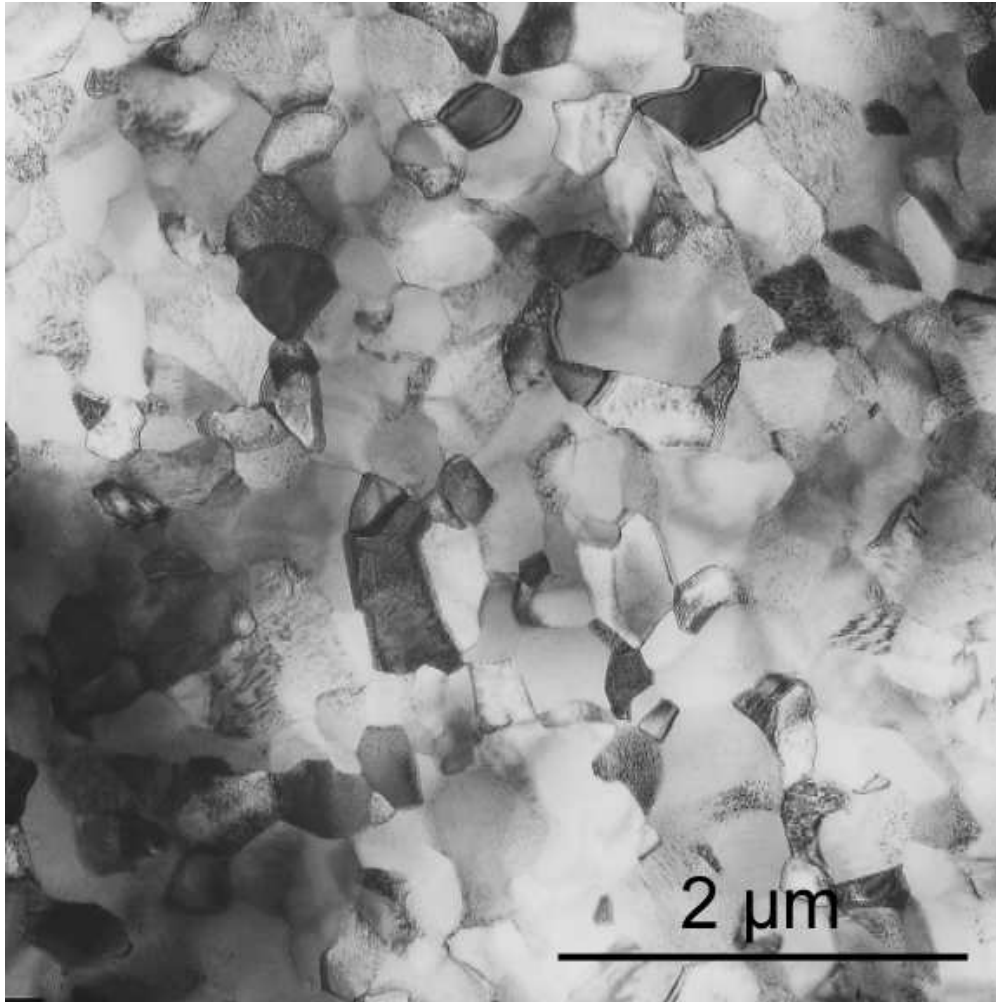
Example of dislocations observed in a specimen deformed at 690°C. All dislocation segments are aligned along 2-fold directions.
46x46mm (600 x 600 DPI)





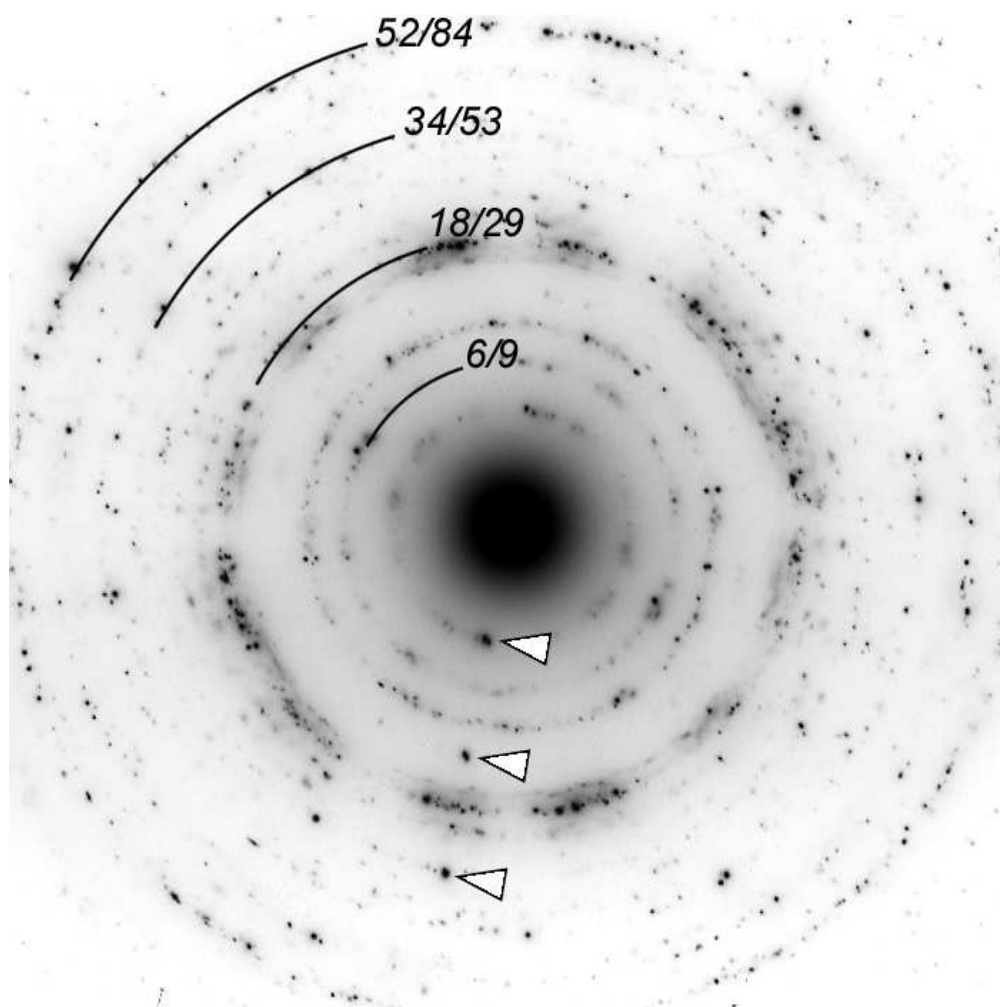
Schematic of the corresponding dislocation configuration. Dislocation segments are lying in a common 5-fold plane, but belong to different glide planes: dislocation segments (1) and (2) have two distinct 3-fold glide planes, segment (3) has a 5-fold glide plane.
 144x107mm (381 x 381 DPI)

1
2
3
4
5
6
7
8
9
10
11
12
13
14
15
16
17
18
19
20
21
22
23
24
25
26
27
28
29
30
31
32
33
34
35
36
37
38
39
40
41
42
43
44
45
46
47
48
49
50
51
52
53
54
55
56
57
58
59
60



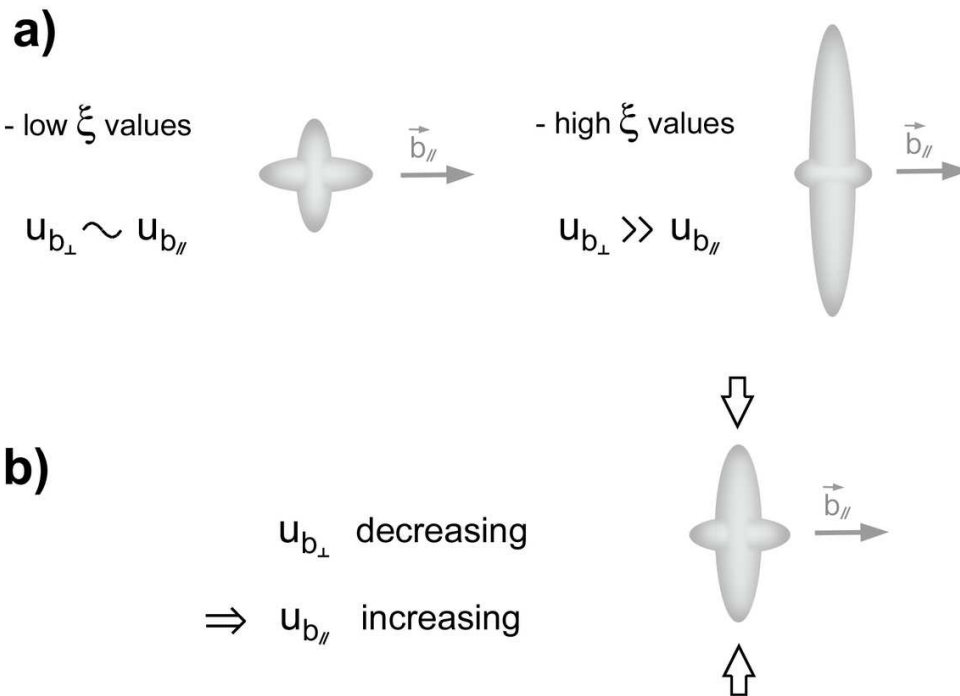
Microstructure of a specimen sheared at 480°C. A microstructure with small disoriented grains is observed.
48x48mm (300 x 300 DPI)





Related selected area electron diffraction pattern. The arrows indicate periodically aligned spots.
59x59mm (300 x 300 DPI)

AMU



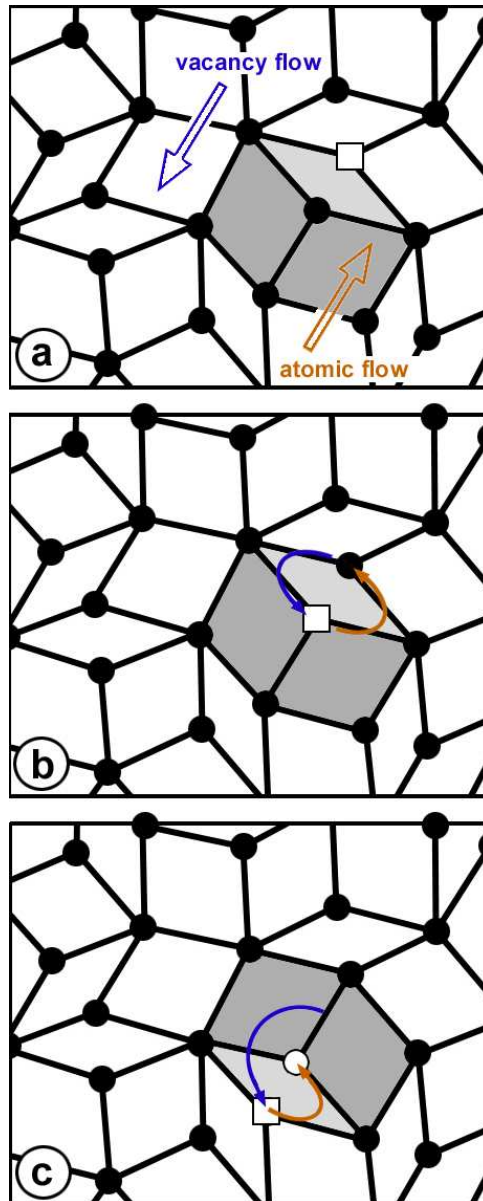
32 Schematic of expected ξ dependences of dislocation core extensions:

- 33 a) Low temperatures.
- 34 • for low ξ values, and displacement fields are similar, leading to almost equivalent core
 - 35 extensions in the glide and climb planes.
 - 36 • for high ξ values, extensions out of the glide plane are predominant, promoting dislocation climb.
- 37 b) High temperatures. With increasing temperatures, due to the phasonic displacement field, the
- 38 geometrically necessary atomic displacements are reduced, leading to a decreasing core extension
- 39 in the climb plane.

40 49x35mm (600 x 600 DPI)

41
42
43
44
45
46
47
48
49
50
51
52
53
54
55
56
57
58
59
60

Only



Diffusion of a vacancy in a 2D-quasiperiodic structure: (a) the vacancy (open square) occupies a node site of the quasiperiodic lattice. (b) The vacancy and one atom exchange their sites. (c) The vacancy moves away to another position of the quasi-lattice, but the atom sits at an intermediate position (open circle). This site does not correspond to an actual node position of the perfect quasiperiodic lattice and represents a so-called phasonic defect, referred to as 'basculon'. In that case, vacancy diffusion enhances phasonic defect nucleation, allowing a reduction in the atomic flux associated with vacancy migration.

58x145mm (200 x 200 DPI)